# On capillary-gravity waves generated by a slow moving object

A. D. Chepelianskii[(a,b)], F. Chevy[(c)] and E. Raphaël[(a)]
[(a)] *Laboratoire Physico-Chimie Théorique, UMR CNRS Gulliver 7083, ESPCI, 10 rue Vauquelin, 75005 Paris, France*
[(b)] *Laboratoire de Physique des Solides, UMR CNRS 8502, Bât. 510, Université Paris-Sud, 91405 Orsay, France and*
[(c)] *Laboratoire Kastler Brossel, ENS, Université Paris 6, CNRS, 24 rue Lhomond, 75005 Paris, France*
(Dated: May 1, 2007)

We investigate theoretically and experimentally the capillary-gravity waves created by a small object moving steadily at the water-air interface along a circular trajectory. It is well established that, for straight uniform motion, no steady waves appear at velocities below the minimum phase velocity $c_{min} = 23\ \mathrm{cm \cdot s^{-1}}$. We show theoretically that no such velocity threshold exists for a steady circular motion, for which, even at small velocities, a finite wave drag is experienced by the object. This wave drag originates from the emission of a spiral-like wave pattern. Our results are in good agreement with direct experimental observations of the wave pattern created by a circularly moving needle in contact with water. Our study leads to new insights into the problem of animal locomotion at the water-air interface.

PACS numbers: 47.35.-i , 68.03.-g



Capillary-gravity waves propagating at the free surface of a liquid are driven by a balance between the liquid inertia and its tendency, under the action of gravity and surface tension forces, to return to a state of stable equilibrium [1]. For an inviscid liquid of infinite depth, the dispersion relation relating the angular frequency $\omega$ to the wave number $k$ is given by $\omega^2 = gk + \gamma k^3/\rho$ where $\rho$ is the liquid density, $\gamma$ the liquid-air surface tension, and $g$ the acceleration due to gravity [2]. The above equation may also be written as a dependence of wave velocity $c = \omega(k)/k$ on wave number

$$c(k) = (g/k + \gamma k/\rho)^{1/2} \tag{1}$$

The dispersive nature of capillary-gravity waves is responsible for the complicated wave pattern generated at the free surface of a still liquid by a moving disturbance such as a partially immersed object (*e.g.* a boat or an insect) or an external surface pressure source [2, 3, 4, 5, 6]. The propagating waves generated by the moving disturbance continuously remove energy to infinity. Consequently, the disturbance will experience a drag, $R_w$, called the *wave resistance* [3]. In the case of boats and large ships, this drag is known to be a major source of resistance and important efforts have been devoted to the design of hulls minimizing it [7]. The case of objects small relative to the capillary length $\kappa^{-1} = (\gamma/(\rho g))^{1/2}$ has only recently been considered [8, 9, 10, 11].

It has been shown [8] that in the case of a disturbance moving at *constant* velocity $\boldsymbol{V}$, the wave resistance $R_w$ cancels out for $V < c_{min}$ where $V$ stands for the magnitude of the velocity and $c_{min} = (4g\gamma/\rho)^{1/4}$ is the minimum of the wave velocity Eq.(1). For water with $\gamma = 73\ \mathrm{mN \cdot m^{-1}}$ and $\rho = 10^3\ \mathrm{kg \cdot m^{-3}}$, one has $c_{min} = 0.23\ \mathrm{m \cdot s^{-1}}$ (room temperature). This striking behavior of $R_w$ around $c_{min}$ is similar to the well-known Cerenkov radiation emitted by a charged particle [12], and has been recently studied experimentally [13, 14]. In this letter, we demonstrate that just like *accelerated* charged particles radiate electromagnetic waves even while moving slower than the speed of light [15], an accelerated disturbance experiences a non-zero wave resistance $R_w$ even when propagating below $c_{min}$. We consider the special case of a uniform circular trajectory, a situation of particular importance for the study of whirligig beetles (*Gyrinidae*, [16]) whose characteristic circular motion might facilitate the emission of surface waves that may be used for echolocation [17, 18].

We consider the case of an incompressible infinitely deep liquid whose free surface is unlimited. In the absence of external perturbation, the free surface is flat and each of its points can be mapped by a radius vector $\boldsymbol{r} = (x, y)$ in the horizontal plane. The motion of a small object along the free surface disturbs the equilibrium position of the fluid, and each of the free surface acquires a finite vertical displacement $\zeta(\boldsymbol{r})$. Rather than solving the complex hydrodynamic problem of finding the flow around a moving object, we consider the displacement of an external pressure source $P_{ext}(\boldsymbol{r}, t)$ [5, 6]. The equations of motion can then be linearized in the limit of small wave amplitudes [19].

In the frame of this linear-response theory, it is convenient to introduce the Fourier transforms of the pressure source $\hat{P}_{ext}(\boldsymbol{k}, t)$ and of the vertical displacement $\hat{\zeta}(\boldsymbol{k}, t)$. The Fourier transform $\hat{P}_{ext}(\boldsymbol{k}, t)$ is related to $P_{ext}(\boldsymbol{r}, t)$ by :

$$P_{ext}(\boldsymbol{r}, t) = \int \frac{d^2k}{(2\pi)^2} e^{i\boldsymbol{k}.\boldsymbol{r}} \hat{P}_{ext}(\boldsymbol{k}, t) \tag{2}$$

(a similar relation exists between $\hat{\zeta}(\boldsymbol{k}, t)$ and $\zeta(\boldsymbol{r}, t)$). It can be shown that, in the limit of small kinematic viscosity $\nu$, the relation between $\hat{\zeta}(\boldsymbol{k}, t)$ and $\hat{P}_{ext}(\boldsymbol{k}, t)$ is given by

$$\frac{\partial^2 \hat{\zeta}}{\partial t^2} + 4\,\nu\,k^2\,\frac{\partial \hat{\zeta}}{\partial t} + \omega^2(k)\,\hat{\zeta} = -\frac{k\hat{P}_{ext}(\boldsymbol{k}, t)}{\rho} \tag{3}$$

In this letter we assume that the pressure source has radial symmetry $P_{ext}(\boldsymbol{r}) = P_{ext}(r)$, and that the trajectory $\boldsymbol{r}_0(t)$ of the object is circular, namely : $\boldsymbol{r}_0(t) = \mathcal{R}\,(\cos(\Omega t), \sin(\Omega t))$. Here $\mathcal{R}$ is the circle radius and $\Omega$ is the angular frequency. The velocity of the object is then given by $V = \mathcal{R}\,\Omega$. These arguments lead to the following time dependence of the applied field $P_{ext}(\boldsymbol{r}, t) = P_{ext}(|\boldsymbol{r} - \boldsymbol{r}_0(t)|)$. In Fourier space, this equation reads $\hat{P}_{ext}(\boldsymbol{k}, t) = \hat{P}_{ext}(k) e^{-i\boldsymbol{k}.\boldsymbol{r}_0(t)}$. Since the right hand side of Eq. (3) is periodic with frequency $\Omega$, it is possible to find its steady state solution by expanding the right hand side into Fourier series. Indeed, the problem becomes equivalent to the response of a damped oscillator to a sum of periodic forces with frequencies $n\Omega$, where $n$ is a positive integer. The vertical deformation at any time $t$ can then be reconstructed by evaluating the inverse Fourier transform. For the particular case of uniform circular motion, the time dependence is rather simple. Indeed, in the steady state regime, the deformation profile rotates with the same frequency $\Omega$ as the moving body. Therefore in the rotating frame $\zeta$ depends on the position on the surface $\boldsymbol{r}$ only. The analytical expression of $\zeta(\boldsymbol{r})$ in cylindrical coordinates $(x, y) = r(\cos\phi, \sin\phi)$ reads :

$$\zeta(r, \phi) = \sum_{n=-\infty}^{\infty} e^{in\phi} \int \frac{k^2 dk}{2\pi\rho} \frac{\hat{P}_{ext}(k) J_n(kr) J_n(k\mathcal{R})}{n^2\Omega^2 - \omega^2(k) + 4in\nu k^2\Omega} \tag{4}$$

where $J_n$ is $n$-th order Bessel function of the first kind. The summation index $n$ is directly related to the $n$-th Fourier harmonic of the periodic function $e^{-i\boldsymbol{k}.\boldsymbol{r}_0(t)}$ : since the problem is linear, the contribution of all the harmonics add together.

The knowledge of the exact structure of the wave pattern is precious, but a quantitative measurement of the wave resistance is needed in order to understand, for example, the forces developed by small animals moving at the surface of water. The force $\boldsymbol{F}(t)$ furnished by the external pressure source is given by : $\boldsymbol{F}(t) = -\int d^2r P_{ext}(\boldsymbol{r}, t) \boldsymbol{\nabla}\zeta(\boldsymbol{r}, t)$ [20]. The wave resistance $R_w(t)$ is defined as the projection of $\boldsymbol{F}(t)$ along the direction of the velocity: $R_w(t) = \boldsymbol{F}(t) \cdot \boldsymbol{V}(t)/V(t)$. For a periodic motion, it is convenient to consider the time-averaged power $P_w = \langle -\boldsymbol{F}(t) \cdot \boldsymbol{V}(t) \rangle$ furnished by the force $\boldsymbol{F}(t)$. One can show that

$$P_w = -\int d^2r \left\langle P_{ext}(\boldsymbol{r}, t) \frac{\partial\zeta(\boldsymbol{r}, t)}{\partial t} \right\rangle \tag{5}$$

This equation reflects the time-averaged power due to the action of the pressure field on the water-air interface [21]. For uniform circular motion, $R_w$ is time independent and is simply given by $R_w = P_w/V$. Combining Eqs. (3) and (5), it is possible to derive an explicit formula for $R_w$:

$$R_w(V, \mathcal{R}) = \sum_{n>0} \frac{n}{\rho\mathcal{R}} \frac{(k_n J_n(k_n\mathcal{R}) \hat{P}_{ext}(k_n))^2}{\left(\frac{d\,\omega^2}{dk}\right)_{k_n}} \tag{6}$$

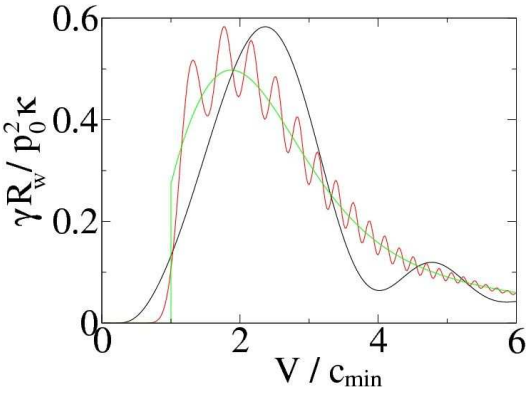


FIG. 1: (Color online) Dependence of the wave resistance $R_w$ as a function of the reduced velocity $V/c_{min} = \mathcal{R}\,\Omega/c_{min}$ for different ratios between the trajectory radius $\mathcal{R}$, and the object size $b$, as predicted by Eq. (6). The red curve (presenting many oscillations) corresponds to $\mathcal{R}/b = 100$, while the black one (with fewer oscillations) corresponds to $\mathcal{R}/b = 10$. The green curve displaying a typical discontinuity at $V = c_{min}$ is the wave drag for a straight uniform motion with velocity $V$ [8]. The object size, $b$, was set to $b = 0.1\,\kappa^{-1}$.

where $k_n$ is the unique solution of the equation $\omega(k_n) = n\,\Omega$ (the notation $R_w(V, \mathcal{R})$ stresses the dependence of $R_w$ on the velocity magnitude and on the trajectory radius). Note that the above equation does not depend of the precise form of the dispersion relation of capillary-gravity waves and thus should be of more general relevance. In deriving Eq. (6), the limit $\nu\kappa/c_{min} \to 0$ was taken (for water, $\nu\kappa/c_{min} \sim 10^{-3}$). Equation (6) shows that the wave resistance $R_w$ takes the form of a sum $R_w = \sum_{n>0} A_n$, where the $A_n$ are positive numbers that measure the contribution of each Fourier mode of the external pressure source (with frequency $n\,\Omega$) to the wave resistance.

The result Eq. 6 differs significantly from the original prediction on the wave drag due to a straight uniform motion with velocity $V$ [8, 11]. Indeed, in this case, for a pressure source with axial symmetry $P_{ext}(r)$, the wave drag $R_{w,l}$ experienced by the object is given by :

$$R_{w,l}(V) = \int_0^{\infty} \frac{kdk}{2\pi\rho} \frac{\hat{P}_{ext}^2(k)\,\theta(V - c(k))}{V^2\sqrt{1 - (c(k)/V)^2}} \tag{7}$$

where $\theta(.)$ is the Heavyside function and $c(k) = \omega(k)/k$ is the phase velocity. The expressions of the wave drag for circular and uniform motion (respectively $R_w(V, \mathcal{R})$ and $R_{w,l}(V)$) are compared on Fig. 1. For the numerical simulations we have assumed the following expression for the pressure source $\hat{P}_{ext}(k) = p_0 \exp(-kb)$. Here $p_0$ is the total force exerted on the surface and $b$ is the typical object size. While all the data shown in this letter are obtained with this expression for $P_{ext}(r)$, we have verified that other distributions (gaussian, step function, ...) lead qualitatively to the same results. Figure 1 shows the value of the reduced wave resistance $\gamma R_w/(p_0^2\kappa)$ as

a function of the reduced velocity $V/c_{min}$ in the limit of large values of $\mathcal{R}/b$. In this regime, one expects the effect of acceleration and curvature to be negligible. We confirmed this behavior by checking numerically that in the limit $\mathcal{R} \to \infty$, $R_w(V,\mathcal{R}) \to R_{w,l}(V)$. However even if the circular wave drag $R_w(V,\mathcal{R})$ is close to $R_{w,l}(V)$ starting from $\mathcal{R}/b \sim 10$, important differences remain even up to very large values of $\mathcal{R}/b$ such as $\mathcal{R}/b \sim 100$. Namely the circular wave drag $R_w(V,\mathcal{R})$ is non zero even for $V < c_{min}$ and is continuous at $V = c_{min}$. Moreover, the wave resistance develops a small oscillating component as a function of the velocity $V$.

The fact that, for a circular motion, the wave resistance is finite even below $c_{min}$ can be understood as follows. In the case of uniform motion all the wavenumbers such as $c(k) < V$ contribute to the wave drag, whereas for circular motion this is the case for only a discrete set of wavenumbers $k_n$. While the condition $c(k) < V$ can be satisfied only when $V > c_{min}$, the equations on the wavenumber $k_n$, $\omega(k_n) = nV/\mathcal{R}$ have positive solutions for any velocity $V$. These wavenumbers $k_n$ create finite contributions $A_n > 0$ to the wave drag. Therefore for a circular trajectory a finite wave drag exists at any velocity $V > 0$, for the same reasons the result is also continuous at $V = c_{min}$. The origin of the oscillations displayed by the wave resistance (see Fig. 1) above $c_{min}$ is related to the oscillatory behavior of Bessel functions and will be analyzed more thoroughly in a future publication.

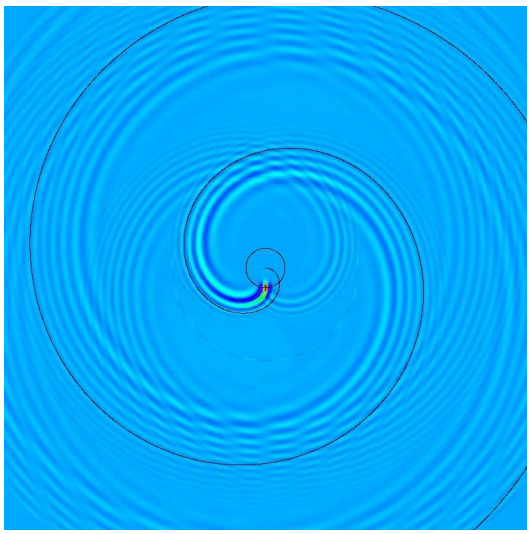

FIG. 2: (Color online) Diagram of the surface deformation $\zeta(\boldsymbol{r})$ for $V/c_{min} = 0.8$, $\kappa\mathcal{R} = 15$ and $\kappa b = 0.1$ as computed numerically from Eq. (4). This image represents a square region of size $400\kappa^{-1}$. The perturbation moves counterclockwise along the black circle and is located at its bottom. The black spiral represents the predicted Archimedean spiral shape of the wave crests with radius given by Eq. (8).

Figure 2 represents the wave crest pattern (computed numerically form Eq.(4)) at the origin of this finite wave drag. It exhibits characteristic concentric Archimedean spirals (also known as arithmetic spirals) of the form $r = a\phi + b$. This can be understood from our theoretical results as follows. In a first estimation, one can assume that the integrals in equation Eq. (4) are dominated by the contribution of the poles at $k = k_n$. Thus $\zeta(\boldsymbol{r})$ can be written as $\zeta(\boldsymbol{r}) \sim \frac{1}{\sqrt{r}} \sum_n B_n e^{i(n\phi - k_n r)}$, where we have used the asymptotic development of $J_n(k_n r)$ at large distances $r$ and $B_n$ are complex coefficients that do not depend on the position $\boldsymbol{r} = r(\cos\phi, \sin\phi)$. By separating the contribution of the different modes in the relation $\boldsymbol{F}(t) = -\int d^2 r P_{ext}(\boldsymbol{r},t)\boldsymbol{\nabla}\zeta(\boldsymbol{r},t)$, one finds that $B_n$ is proportional to $A_n$ (where, as defined earlier, the positive coefficients $A_n$ measure the contribution of each Fourier mode to the wave drag: $R_w = \sum_{n>0} A_n$). One can show that in the regime of small object sizes $\kappa b \ll 1$, the proportionality constant between $B_n$ and $A_n$ depends only weakly on the Fourier mode number $n$; thus, one has $\zeta(\boldsymbol{r}) \propto \frac{1}{\sqrt{r}} \sum_n A_n e^{i(n\phi - k_n r)}$. We have checked numerically that in the regime $V < c_{min}$, the distribution of the coefficients $A_n$ is usually peaked around $n \sim \kappa\mathcal{R}$. For example, for $\kappa\mathcal{R} = 10$ and $\kappa b = 0.1$, $A_n$ is peaked around $n = 10$ for velocities $V$ in the interval $(c_{min}/2, c_{min})$. The wave-crests are given by the lines of constant phase $n\phi - k_n r = const$ of the dominant mode $n = \kappa\mathcal{R}$, leading to the following expression:

$$a \approx \frac{\kappa\mathcal{R}}{k(\omega = \kappa V)} \tag{8}$$

where $k(\omega)$ is the inverse function of $\omega(k)$. An interesting special case of the formula Eq. (8) corresponds to $V = c_{min}$, for which one obtains $a \approx \mathcal{R}$. The spiral predicted by Eq. (8) is in very good agreement with the exact numerical results (Eq. (4)), as can be seen in Fig. 2.

We have also compared our theoretical approach with experimental results obtained using a one millimeter wide stainless steel needle immersed in a 38 cm wide water bucket. The needle was rotated on circular trajectories of various radii and angular velocities. A typical wave pattern obtained by this method is shown on Fig. 3 for $\mathcal{R} \approx 2.7$cm and $\Omega \approx 2\pi \times 1.2\,$Hz (corresponding to $V/c_{min} \approx 0.9$) and unambiguously demonstrates the existence of a wake at velocities smaller than $c_{min}$. The observed wave pattern is in remarkable agreement with the theoretical prediction $r = a\phi + b$ with $a$ given by Eq. (8) and $b$ a free parameter corresponding to an overall rotation of the spiral [22]. For $V/c_{min}$ lower than 0.8, no wake was observed by naked eye. At lower rotation velocities, we probed the surface deformation by measuring the deflexion of a laser beam reflected by the air-water interface at a distance $r = 11$ cm from the rotation axis. Using this scheme, we have established the existence of waves down to $V/c_{min} \approx 0.6$ below which the signal to noise ratio of the experiment becomes to small to observe the laser deflection. Note that this value is in qualitative agreement with Fig. 1 where the wave resistance (hence the wave amplitude) has also significatively decreased with respect to its maximum value for $V/c_{min} \lesssim 0.5$.

FIG. 3: (Color online) Photography of the wave crests generated on a water surface by a needle rotating counterclockwise along a circular trajectory (radius $\mathcal{R} \approx 2.7\,\mathrm{cm} \approx 9\,\kappa^{-1}$) with a velocity $V \approx 21\,\mathrm{cm}\cdot\mathrm{s}^{-1} \approx 0.9\,\mathrm{c_{min}}$. The black curve represents the predicted Archimedean spiral with radius $a$ given by Eq. (8).

To summarize, we have shown theoretically that a disturbance moving along a circular trajectory experienced a wave drag even at angular velocities corresponding to $V < c_{min}$, where $c_{min}$ is the minimum phase velocity of capillary-gravity waves. Our prediction is supported by experimental observation of a long distance wake for $V/c_{min}$ as low as 0.6. For $V/c_{min} > 0.8$, we observed by naked eye Archimedean spiral shaped crests, in good agreement with theory. These results are directly related to the accelerated nature of the circular motion, and thus do not contradict the commonly accepted threshold $V = c_{min}$ that is only valid for a rectilinear uniform motion, an assumption often overlooked in the literature. It would be very interesting to know if whirligig beetles can take advantage of such spirals for echolocation purposes. More generally, the results presented in this letter should be important for a better understanding of the propulsion of water-walking insects [23, 24, 25, 26] where accelerated motions frequently occurs (*e.g* when hunting a prey or escaping a predator [27]). Even in the case where the insect motion is rectilinear and uniform, one has to keep in mind that the rapid leg strokes are accelerated and might produce a wave drag even below $c_{min}$.

We are grateful to Jérôme Casas and José Bico for fruitful discussions. F.C. acknowledges support from Région Ile de France (IFRAF) and A.C. acknowledges support from Ecole Normale Supérieure Paris.

[1] L. D. Landau and E. M. Lifshitz *Fluid Mechanics*, 2nd ed. (Pergamon Press, New York 1987).
[2] D. J. Acheson, *Elementary Fluid Dynamics* (Clarendon Press, Oxford,1990).
[3] J. Lighthill, *Waves in Fluids*, 6th ed. (Cambridge University Press, Cambridge, 1979).
[4] H. Lamb, *Hydrodynamics*, 6th ed. (Cambridge University Press, Cambridge, 1993).
[5] Lord Rayleigh, Proc. London Math. Soc., **15**, 69 (1883).
[6] Lord Kelvin, Proc. London Math. Soc. A, **15**, 80 (1887).
[7] J. H. Milgram, Annu. Rev. Fluid Mech., **30**, 613 (1998).
[8] E. Raphaël and P.-G. de Gennes, Phys. Rev. E, **53**, 3448 (1996).
[9] D. Richard and E. Raphaël, Europhys. Lett. **48**, 53 (1999).
[10] S.-M. Sun and J. Keller, Phys. Fluids, **13**, 2146 (2001).
[11] F. Chevy and E. Raphaël, Europhys. Lett., **61**, 796 (2003).
[12] P. A. Cherenkov, C. R. Acad. Sci. URSS **8**, 451 (1934).
[13] J. Browaeys, J.-C. Bacri, R. Perzynski and M. Shliomis, Europhys. Lett. **53**, 209 (2001).
[14] T. Burghelea and V. Steinberg, Phys. Rev. Lett. **86**, 2557 (2001) and Phys. Rev. E **66**, 051204 (2002).
[15] J. D. Jackson, *Classical Electrodynamics*, 3rd ed. (Wiley, 1998).
[16] W. Nachtigall, in *The Physiology of Insecta* (Academic Press, New York, 1965)
[17] V. A. Tucker, Science **166**, 897 (1969).
[18] M. W. Denny, *Air and Water*, (Princeton University Press, Princeton 1993).
[19] For nonlinear effects, see F. Dias and C. Kharif, Annu. Rev. Fluid Mech., **31**, 301 (1999).
[20] T. H. Havelock, Proc. R. Soc. A, **95**, 354 (1918).
[21] We have assumed that the shape of the pressure source is time independent.
[22] Note that we also observed on some pictures the weaker spiral seen in Fig. 2 propagating in the opposite direction with respect to the main wake. This "advanced" wake could only be observed at high velocities ($V/c_{min} \sim 2$) because of its small relative amplitude.
[23] R. McNeill Alexander, *Principle of Animal Locomotion*, (Princeton University Press, Princeton 2002).
[24] J. W. Bush and D. L. Hu, Annu. Rev. Fluid Mech., **38**, 339 (2006).
[25] M. W. Denny, J. Exp. Biol., **207** 1601 (2004).
[26] O. Buhler, J. Fluid Mech., **573**, 211 (2007).
[27] H. Bendele, J. Comp. Physiol. A, **158**, 405 (1986).